A discussion for the formation of cassie droplet on nanostructured surface using molecular dynamics simulation

Dong Niu [a], Hongtao Gao [a,*], Yuying Yan [b]

[a] *Institute of Refrigeration & Cryogenics Engineering, Dalian Maritime University, Dalian, 116026, PR China*
[b] *Fluids & Thermal Engineering Research Group, Faculty of Engineering, University of Nottingham, University Park, Nottingham, NG7 2RD, UK*

ARTICLE INFO	ABSTRACT
	Dropwise condensation has attracted a large amount of attention due to its higher heat transfer coefficient than filmwise condensation. Droplet nucleation and growth have a significant influence on droplet state in condensation process. In this study, the molecular dynamics simulation is performed to investigate the dropwise condensation on different nanostructured surfaces. For the nanostructured surface with a high aspect ratio, all the droplets nucleate and grow inside the rough structures. Decreasing the center distance of nanostructures or increasing the heat flux could lead to a preferential growth on the up section of the nanostructures. Furthermore, the effect of droplet growth and coalescence on the transition from Wenzel state to Cassie state is investigated for a large-scale system. The simulation results show that three typical droplet state transition mode corresponding to the heat flux could be obtained.

1. Introduction

Condensation heat transfer is a common phase-change process in nature [1–3]. Dropwise condensation mode has been widely studied due to its higher heat transfer coefficient and its potential applications in many fields such as power generation [4], water desalination [5], thermal management of electronics [6] and water harvesting [7,8].

In general, microtextured or nanotextured hydrophobic surfaces can transform into superhydrophobic state like lotus leaves which is the key to realize the dropwise condensation heat transfer enhancement. In recent years, with the development of nanofabrication, nanostructured surfaces have been widely used in dropwise condensation heat transfer [9–11]. However, when a droplet is placed on a nanostructured surface, two different wetting states can be presented. If the droplet could suspend on the nanostructures, it exhibits the Cassie state [12], otherwise the droplet is penetrated by the nanostructures and shows the Wenzel state [13]. Different from the process of water harvesting from fog in nature, the droplet in dropwise condensation will undergo the growth process from the nanoscale to macroscale. The interaction between the droplet and nanostructures is very complicated in this multiscale process. Droplet behavior including the nucleation, wetting state, dynamic mode transition, coalescence-induced droplet jumping is the research focus for dropwise condensation heat transfer on nanostructured surface. Certainly, the Cassie droplet state is preferred for dropwise condensation heat transfer enhancement due to its smaller contact angle hysteresis. However, one of the intractable problems for nanostructured surface is that a sable Cassie state is particularly difficult to achieve which requires harsh conditions. The dropwise condensation on nanostructured surface under high supersaturation or subcooling degree will easily lead to the pinned Wenzel state

---

and the droplet is hard to departure which could bring the flooding condensation mode. Miljkovic et al. [14] experimentally demonstrated that jumping condensation could be replaced by flooding condensation under high supersaturation, which degraded the condensation heat transfer coefficient by 40% compared to the dropwise condensation on smooth surface.

About the formation of Wenzel droplet (flooding mode) in dropwise condensation process, there have been many studies in revealing the physical nature of this phenomenon. The role of local energy barriers and structure length scale was elucidated by Enright et al. [15] in which a mechanistic framework was presented to explain the complex nature of water condensation on structured surfaces. This local energy barriers could be overcome via nucleation-mediated droplet-droplet interactions which further lead to the wetting states transition. The high subcooling degree (large nucleation density) will result in growth and merging of multiple droplets in a unit cell, consequently, the energy barrier of droplet lateral growth inside the rough structure is overcome where the Wenzel state droplet will appear. In our previous study [16], the droplet nucleation and growth on a rough surface was investigated using the molecular dynamics simulation. The simulation results indicate that the high heat flux could lead to droplet nucleation and growth inside the rough structure and finally a Wenzel droplet will form due to the coalescence between the inside droplet and the initial existing droplet. However, the initial existing droplet was arranged in all simulations to assume that the droplet would nucleate at the top of rough structure firstly. Wen et al. [17] experimentally studied the dropwise condensation heat transfer on a nano-wired hydrophobic surface. Based on the experimental results, the spatial control on droplet nucleation and wetting state was proposed in which the droplet cannot nucleate inside the nanowires due to the low vapor density and high nucleation barrier. Lv et al. [18] reported an *in situ* observation of condensation on micro-nanostructured superhydrophobic surfaces using optical microscopy. It is found that individual droplets preferentially nucleate at the top and the edge of single micropillars and emphasized that the formation of the Cassie droplet is the result of a continuous coalescence of individual small droplets. Therefore, according to the previous viewpoint, whether the droplet nucleation inside the nanostructures occurs or not is controversial and the effect of coalescence on the formation of Wenzel droplet or Cassie droplet is still not clear.

Actually, although a large number of experiments have been carried out on the droplet nucleation and growth, it is almost impossible to directly observe droplet nucleation on nanostructured surfaces due to the magnitude of the critical nucleation size [19–21]. Molecular dynamics simulation is an effective method and has been widely used to investigate droplet nucleation and growth in previous study. Kimura and Maruyama [22] investigated the droplet nucleation on the solid surface using molecular dynamics simulation. The nucleation rate, nucleation size and the required free energy agreed well with classical heterogeneous theory for the smaller cooling rate. The initial stage of condensation for different surface wettability was investigated using molecular dynamics simulation [23]. Different condensation modes including the no-condensation, dropwise condensation and filmwise condensation were quantitatively analyzed in the simulation. Niu et al. [24] obtained the reasonable nucleation information including the critical radius and nucleation density considering the effect of liquid-solid interfacial thermal resistance determined by the molecular dynamic simulation. Furthermore, a new dropwise condensation heat transfer model was established based on the modified nucleation information. Gao et al. [25] performed molecular dynamics simulation to investigate the effect of solid fraction on droplet wetting state and condensation, showing that droplets exhibit the Cassie state on nanostructured surface with a high fraction of solid surface and gradually transforms into the Wenzel state when the fraction of the solid surface decreases.

Although a large number of experiments and simulations have been carried out on the droplet behavior, the relationship between the droplet wetting state and nucleation or growth on the nanostructured surface is still not clear in the nanoscale. In this work, we
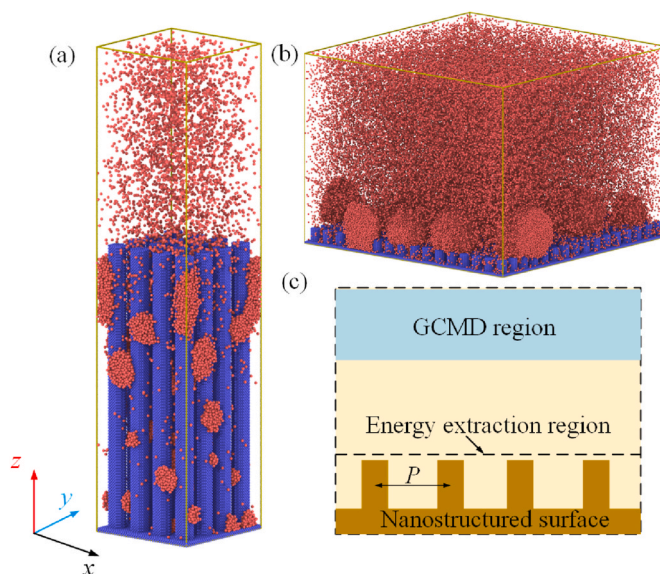

Fig. 1. The setup of the simulation system. (a) Nano-wired surface with a high aspect ratio, (b) Large scale simulation system, (c) Region setup to achieve condensation.

perform the molecular dynamics simulation to study the droplet nucleation and growth on the nano-wired surface with a high aspect ratio in which Wen et al. [17] suggested that the Cassie droplet only nucleated at the top of nanostructures under small subcooling degree. The effects of surface wettability, nanostructure spacing, and heat flux are discussed in detail. Furthermore, the large scale simulations of dropwise condensation on the nanostructured surface for different heat flux are carried out to directly demonstrate how the nucleation density and droplets interaction to determine the droplet wetting state from the point of nucleation and initial growth of droplet.

This paper is organized as follows. In Section 2, the simulation method and details are introduced and in Section 3, the results of dropwise condensation on nanostructured surface is presented. Finally, Section 4 gives a conclusion.

2. Simulation details

Molecular dynamics simulation in this work is performed using the LAMMPS package [26]. In the first part of the work, the nanostructured surface with a high aspect ratio is built firstly. In the x and y directions, the periodic boundary condition is used. At the top of z direction for the simulation system, the reflection boundary is applied. The setup of the simulation system is shown in Fig. 1a including the Argon atoms and Pt-like nanostructured surface with the 4×4 array. The solid surface is a face-centered cubic crystal with a lattice constant $S = 3.92$ Å. The diameter and height of the nanopillar are fixed at $6S$ and $100S$, respectively. The center distance (P), the intrinsic contact angle and the extracted heat flux will be adjusted for the nanostructured surface with a high aspect ratio. To investigate the effect of droplet growth on the wetting state during the condensation process, a large simulation (16×16 array) system with the three dimensions of $62.7 \times 62.7 \times 47$ nm in the x, y and z directions is built as shown in Fig. 1b in which the diameter, height and center distance of nanostructure are fix at $10S$, $12S$, and $14S$, respectively. Only the extracted heat flux is adjusted to create different nucleation density and droplet growth mode.

The Lennard-Jones 12–6 potential, $E = 4\varepsilon_{ij}\left[\left(\frac{\sigma_{ij}}{r_{ij}}\right)^{12} - \left(\frac{\sigma_{ij}}{r_{ij}}\right)^6\right]$, is used to describe the interaction between argon atoms in which $\varepsilon = 0.2381$ Kcal/mol and $\sigma = 3.405$ Å are the characteristic energy and the van der Waals radius, respectively. The atoms of the Pt-like rough surface is fixed as a rigid body. The interaction between the solid surface and the argon atoms is also described using the 12-6 LJ potential with the $\varepsilon = 0.071$ Kcal/mol and $\sigma = 2.94$ Å. This interaction parameters represents a general intrinsic contact angle about 112° for a hydrophobic surface. The details of contact angle calculation are same as our previous study [24].

Fig. 1c shows the setup of the simulation domain in the condensation process. The GCMD (the combination of Grand Canonical
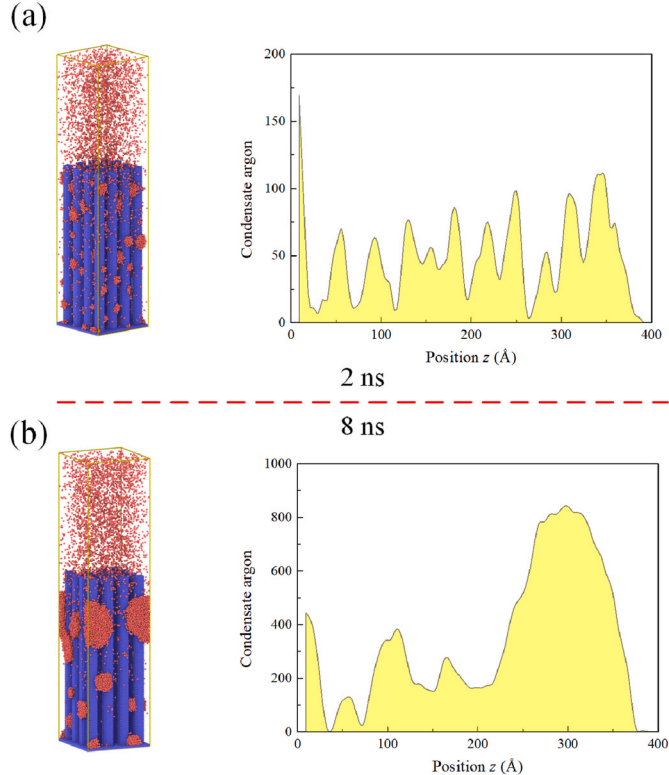

Fig. 2. Condensation snapshots and condensate distribution in the z direction ($P = 10S$, Heat flux $= 0.0025$Kcal·mol^{-1}·fs^{-1}). (a) Time $= 2$ ns, (b) Time $= 8$ ns.

Monte Carlo method and molecular dynamics simulation) region with a thickness of 20S in the z direction could provide stable temperature and pressure control as the heat source. The heat flux is extracted from the argon atoms in the bottom of simulation domain to as the heat sink where the dropwise condensation is induced. All simulations are performed in two stages. In the first stage, the temperature and pressure in GCMD region is maintained at 110 K and 6.5 atm using the Grand Canonical Monte Carlo method and molecular dynamics simulation. The NVT ensemble is used for the whole simulation domain until the system reaches equilibrium state for 10 ns with a timestep of 5 fs. The argon atoms can be displaced, deleted, or created every 100 steps. The insertion or deletion for argon atoms are equal probability in the GCMD region judged by the usual criteria of the Grand Canonical Monte Carlo algorithm. Then, the NVT ensemble is removed from the vapor atoms, the NVE ensemble is employed and the setup of Grand Canonical Monte Carlo in the GCMD region remains the same. The heat flux is extracted in the regions of heat sink which promote the droplet nucleation and growth.

3. Results and discussion

3.1. The nanostructured surface with high aspect ratio

Fig. 2 shows the droplet nucleation and growth during the condensation process on the rough surface of $P = 10S$, Heat flux = 0.0025 Kcal mol^{-1}·fs^{-1}. In order to quantitatively observe the droplet nucleation and growth characteristics, the cluster analysis is performed according to the Stillinger criterion [27,28]. A cluster is defined as a set of atoms within the cutoff distance of 3.825 Å [29] from one or more other atoms and all clusters are sorted by the size. The simulation domain is divided into 120 slabs in the z direction to obtain the spatial distribution of condensate. At the initial stage of condensation (0–2 ns), the cluster gradually form and increases as shown in Fig. 2. Based on the analysis of condensate spatial distribution as shown in Fig. 2, we can find that the droplets present an almost uniform distribution in the z direction at the stage of 0–2 ns. However, with the continuous condensation, the differentiated droplet growth leads to a nonuniform distribution of condensate in the z direction. The simulation results proved that the droplets nucleated in the upper section of nanostructures will grow up with priority. On the contrary, the droplet growth near the bottom is inhibited as shown in Fig. 2. The occurrence of droplet growth near the bottom requires the supplement of vapor atoms from outside. The inflow atoms will firstly flow across the top of the rough structures. Under current condensation conditions, the inflow vapor atoms will contact the existing droplet in the upper section and condense directly with a higher probability, which effectively restricts the droplet growth near the bottom.
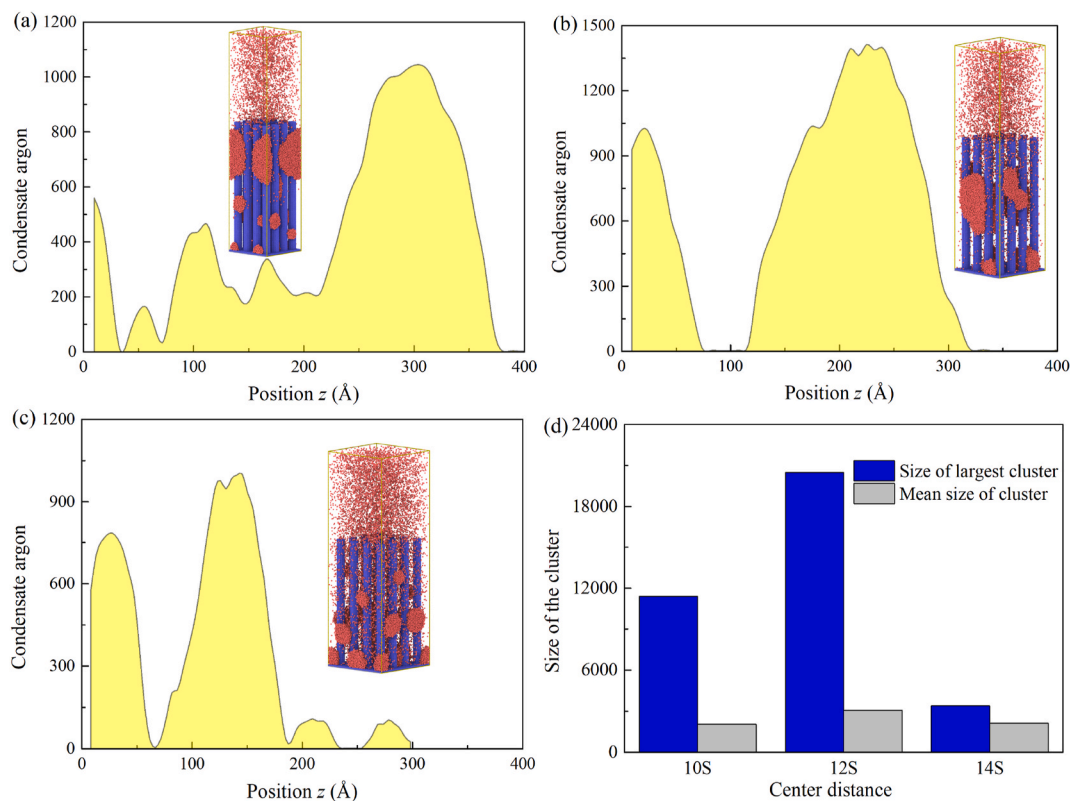

Fig. 3. Condensation snapshots and condensate distribution in the z direction at 10 ns for different center distance (Heat flux = 0.0025 Kcal mol^{-1}·fs^{-1}), (a) $P = 10S$, (b) $P = 12S$, (c) $P = 14S$, (d) Differentiated droplet growth mode.

Then, the effect of center distance P on the droplet nucleation and growth under the same heat flux of 0.0025 Kcal mol^{-1}·fs^{-1} is investigated. Fig. 3 shows the condensation snapshot at 10 ns for different center distance P. From the simulation results, we can find that the condensate gradually moves down in the z direction as the as the center distance increases. It is proved that the dense nanostructures could result in droplet preferential growth in the upper section of nanostructures. We track the size (atoms number for the cluster) variation of the condensate droplet during the condensation process. As shown in Fig. 3d, the size of the largest droplet and the mean size of all condensate droplets at 10 ns inside the nanostructures are counted. Compared with the results of $P = 10S$ and $P = 12S$, the differentiated growth for $P = 14S$ is transformed into a homogeneous mode. This is because the mass transfer resistance of vapor atoms is decreased with the increase of center distance between two nanostructures. Consequently, it will be easy for the sparse nanostructures to transport vapor atoms to the bottom which would lead to a uniform growth of the condensate droplets.

A multitude of experimental study have already proved that large subcooling degree or heat flux could lead to the nucleation-induced flooding condensation. For the nano-wired surface with a high aspect ratio, Wen et al. [17] suggested that the Cassie droplet only nucleated at the top of nanostructures under small subcooling degree. In this work, different heat fluxes ranging from 0.0009 to 0.0055 Kcal mol^{-1}·fs^{-1} are applied on the vapor atoms in the heat sink region. We consider the case that the center distance P is fixed at 12S.

Fig. 4 shows the condensation snapshot at 10 ns for different heat flux. Under the heat flux of 0.0009 Kcal mol^{-1}·fs^{-1}, we can observe that the nucleated droplets are mainly distributed in the middle and bottom section of the nanostructures with a uniform size. As the heat flux increases, the vapor atoms are more likely to condense at upper section of nanostructures. The differentiated growth mode in the z direction occurs in which the larger droplets grow at the upper section and the growth of droplets located at the bottom are suppressed. Fig. 4 also shows the mass center distribution for the total condensate and the largest droplet in the z direction for different heat flux in which we can precisely indicate that the high heat flux would lead to a preferential droplet growth at the up section. The differentiated growth mode is mainly caused by two reasons. Firstly, the high heat flux (large subcooling degree) could make the condensation to occur more easily according to the classical nucleation theory. The incoming vapor atoms are enriched at the up section and the vapor located at the bottom is relatively rarefied before condensation. Therefore, the droplet nucleation is more likely to occur at the up section. Secondly, after droplet nucleation, the inflow vapor atoms will firstly flow across the top of the rough structure. The inflow saturated vapor atoms will contact with the existing droplet and condense directly with a higher probability.

To summarize, in all simulations considering the effect of center distance and heat flux, all the droplets are formed inside the rough structures. However, the Cassie droplet nucleated above the nanostructures does not appear which is inconsistent with the previous study [17] about the formation of Cassie droplet on the nano-wired surface. We suppose that this situation may be caused by two factors. Firstly, due to the limitation of simulation capacity, the size of nanostructures used in the molecular dynamic method is still much smaller than the actual size which is almost equivalent to the nucleation size of droplet. Therefore, the droplet nucleation above the nanostructures is particularly difficult under such a simulation condition. Secondly, the interaction between droplet or growth of droplet itself should be considered when discussing the formation of Cassie droplet rather than just considering the nucleation location. The growth-induced or coalescence-induced Cassie droplet during the condensation process should also be investigated in detail. In the next section, the simulation results for a large simulation system will give some explanation about the effect of droplet growth and coalescence on the droplet state transition during the condensation process.

3.2. The effect of droplet growth and coalescence

Fig. 5 shows the droplet growth and coalescence during the condensation process in a large simulation (16 × 16 array) system. Due to the small rough structure in molecular dynamics method, it is easy to nucleate at the bottom of the rough structure firstly. However,
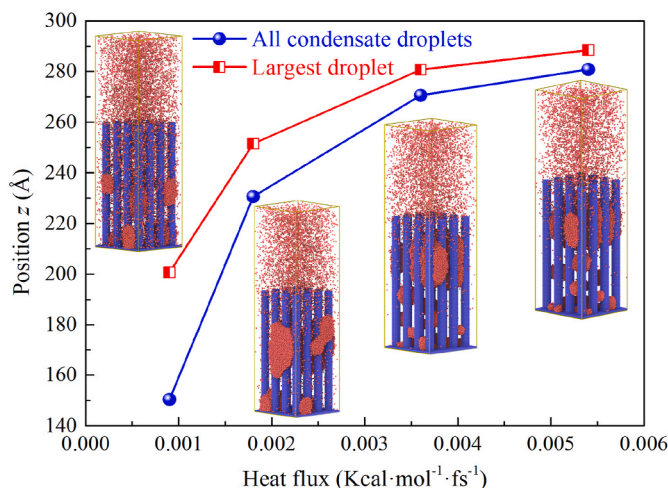

Fig. 4. Condensation snapshots and mass center distribution of condensate in the z direction for different heat flux at 10 ns ($P = 12S$).

the droplet transition from Wenzel state to the Cassie state with a different size can be achieved as circled in Fig. 5. The variation of droplet number is counted by the cluster analysis with the droplet growth and coalescence as shown in Fig. 6. When there exists a large heat flux, more droplets will be generated on the nanostructured surface due to the lower nucleation barrier. The large nucleation density will result in growth and coalescence of multiple droplets per unit area. Therefore, the dramatical fluctuations for droplet number will be presented under a large heat flux. In contrast, for the lower heat flux, the variation of droplet number is gently changed relatively. Especially for the case of 0.002 Kcal mol^{-1}·fs^{-1}, the long plateau will be appeared during the condensation process which proved that the single droplet growth mode dominates the initial condensation stage.

Based on the cluster analysis during the condensation process under different heat flux, we can find three typical droplet state transition mode. For the large heat flux, due to the larger nucleation density, the coalescence-induced transition from Wenzel state to Cassie state is the dominant pattern. It is remarkable that for this transition mode the droplet coalescence occurs inside the rough structures at the initial stage which could make the energy barrier be overcome and lead to a droplet laterally growth. When coalescing to a certain extent, the coalescence between the droplets far enough apart could achieve the state transition from Wenzel state to Cassie state. Secondly, for a lower heat flux, the direct condensation of vapor atoms is the main driving force to realize the droplet state transition. In such a situation, as the droplet growth continues, the restricted droplet becomes deformed, and the Laplace pressure difference is generated inside the droplet which contributes to overcoming the pinning effect from the nanostructures. Finally, for a medium heat flux such as the 0.004 Kcal mol^{-1}·fs^{-1}, the single droplet growth and coalescence would work together to achieve the droplet state transition within a long enough condensation time. Fig. 7 shows the size variation of the first droplet before and after state transition which could more directly indicate the mechanism of three modes.

The critical droplet size to realize the state transition is calculated under different heat flux as shown in Fig. 8. For this nano-structured surface with an intrinsic contact angle of 112°, the apparent contact angle could be obtained according to the Cassie-Baxter equation, $\cos \theta^* = f \cos \theta + f - 1$, where the f is the solid area fraction of the substrate contacting the droplet. Based on the setup of the nanostructures, the apparent contact angle of 145.4° could be obtained and used to calculate the droplet diameter combining the
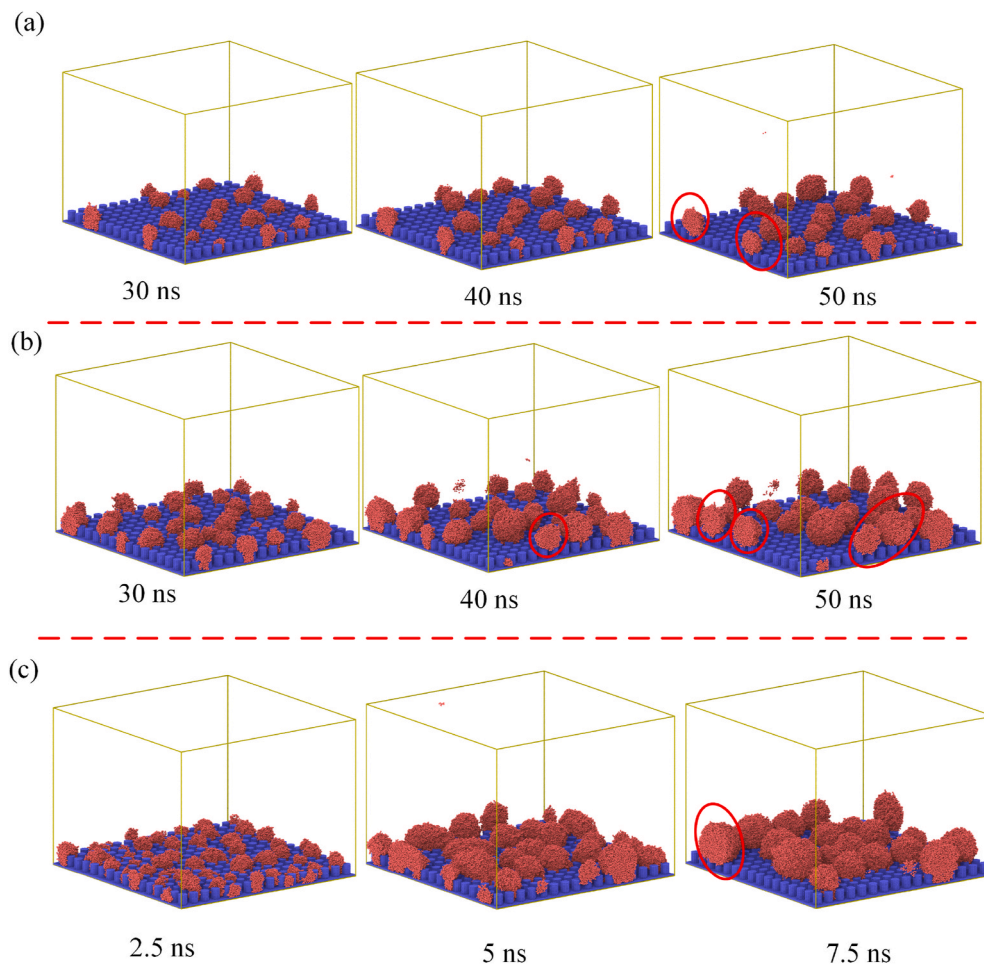

Fig. 5. Snapshots of droplet growth and coalescence for large scale simulation system. (a) Heat flux = 0.002 Kcal mol^{-1}·fs^{-1}, (b) Heat flux = 0.004 Kcal mol^{-1}·fs^{-1}, (c) Heat flux = 0.016 Kcal mol^{-1}·fs^{-1}.
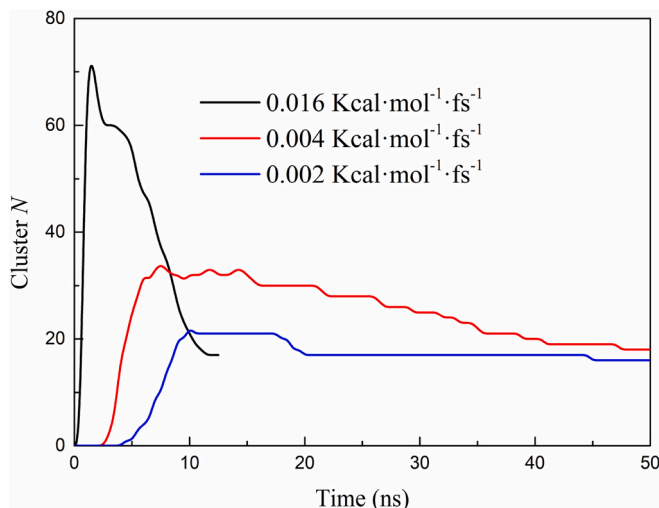
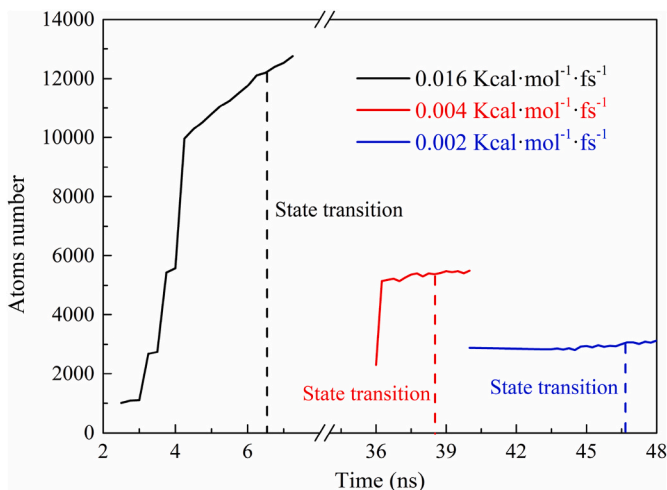**Fig. 6.** Cluster analysis during the condensation process.

Fig. 7. Size variation of the first droplet before and after state transition.

volume formula. As shown in Fig. 8, the critical droplet size is gradually increased with the increase of heat flux which is a result of different transition mode as discussed above.

The dropwise condensation on nanostructured surface under high supersaturation or subcooling degree will easily lead to a flooding condensation mode. It is worth noting that in our molecular dynamic simulations the transition from Wenzel state to Cassie state could be always achieved for different heat flux. This is because that the rough structures used in the simulation is much smaller than the real rough structures used in the experiment. Even so, we are still able to get some valuable laws and mechanisms by analogy. The droplet wetting state in the dropwise condensation process is determined by multiple factors including the setup of rough structures, condensation condition and so on. The transition from Wenzel state to Cassie state is not only affected by the nucleation location but also dominated by the growth of droplet itself or the coalescence.

4. Conclusions

In this work, we have investigated droplet nucleation and growth characteristics on nanostructured surfaces using the molecular dynamics simulation. The mechanism of droplet state transition during condensation process is discussed in detail from the nanoscale.

For the condensation on the nanostructured surface with a high aspect ratio, all the droplets nucleate and grow inside the rough structures. The simulation results show that decreasing the center distance of nanostructures or increasing the heat flux could lead to a preferential growth on the up section and the droplet at the bottom will be suppressed. Furthermore, the effect of droplet growth and coalescence on the transition from Wenzel state to Cassie state is investigated in a larger simulation system. Three typical droplet state
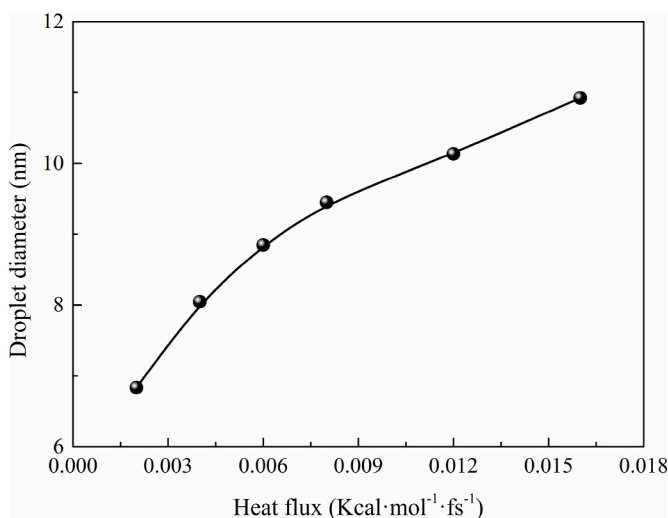
Fig. 8. Critical size for the droplet state transition.

transition mode corresponding to the heat flux could be obtained. It is our hope that these findings could encourage a clear under-standing of droplet dynamic wetting mechanism and provide guidance for the surface optimal design which can serve to further enhance condensation heat transfer.

Author statement

Professors Gao and Yan proposed the idea for the study, and Doctor Niu performed simulations. All authors read and contributed to the manuscript.

Declaration of competing interest

The authors declare that they have no known competing financial interests or personal relationships that could have appeared to influence the work reported in this paper.

Acknowledgments

References

[1] A.R. Parker, C.R. Lawrence, Water capture by a desert beetle, Nature 414 (2001) 33.
[2] Y. Zheng, H. Bai, Z. Huang, et al., Directional water collection on wetted spider silk, Nature 463 (2010) 640–643.
[3] K.C. Park, P. Kim, A. Grinthal, et al., Condensation on slippery asymmetric bumps, Nature 531 (2016) 78–82.
[4] D. Attinger, C. Frankiewicz, A.R. Betz, et al., Surface engineering for phase change heat transfer: a review, MRS Energy Sustain. 1 (2014).
[5] A.D. Khawaji, I.K. Kutubkhanah, J.M. Wie, Advances in seawater desalination technologies, Desalination 221 (2008) 47–69.
[6] J.B. Boreyko, Y. Zhao, C.H. Chen, Planar jumping-drop thermal diodes, Appl. Phys. Lett. 99 (2011) 234105.
[7] A. Lee, M.W. Moon, H. Lim, et al., Water harvest via dewing, Langmuir 28 (2012) 10183–10191.
[8] H.G. Andrews, E.A. Eccles, W.C.E. Schofield, et al., Three-dimensional hierarchical structures for fog harvesting, Langmuir 27 (2011) 3798–3802.
[9] H.W. Hu, G.H. Tang, D. Niu, Experimental investigation of condensation heat transfer on hybrid wettability finned tube with large amount of noncondensable gas, Int. J. Heat Mass Tran. 85 (2015) 513–523.
[10] B. Peng, X. Ma, Z. Lan, et al., Experimental investigation on steam condensation heat transfer enhancement with vertically patterned hydrophobic–hydrophilic hybrid surfaces, Int. J. Heat Mass Tran. 83 (2015) 27–38.
[11] H.W. Hu, G.H. Tang, D. Niu, Experimental investigation of convective condensation heat transfer on tube bundles with different surface wettability at large amount of noncondensable gas, Appl. Therm. Eng. 100 (2016) 699–707.
[12] A.B.D. Cassie, S. Baxter, Wettability of porous surfaces, Trans. Faraday Soc. 40 (1944) 546–551.
[13] R.N. Wenzel, Resistance of solid surfaces to wetting by water, Ind. Eng. Chem. 28 (1936) 988–994.
[14] N. Miljkovic, R. Enright, Y. Nam, et al., Jumping-droplet-enhanced condensation on scalable superhydrophobic nanostructured surfaces, Nano Lett. 13 (2013) 179–187.
[15] R. Enright, N. Miljkovic, A. Al-Obeidi, et al., Condensation on superhydrophobic surfaces: the role of local energy barriers and structure length scale, Langmuir 28 (2012) 14424–14432.

[16] D. Niu, G.H. Tang, Molecular dynamics simulation of droplet nucleation and growth on a rough surface: revealing the microscopic mechanism of the flooding mode, RSC Adv. 8 (2018) 24517–24524.

[17] R. Wen, Q. Li, J. Wu, et al., Hydrophobic copper nanowires for enhancing condensation heat transfer, Nano Energy 33 (2017) 177–183.

[18] C. Lv, P. Hao, X. Zhang, et al., Dewetting transitions of dropwise condensation on nanotexture-enhanced superhydrophobic surfaces, ACS Nano 9 (2015) 12311–12319.

[19] X. Liu, P. Cheng, Dropwise condensation theory revisited: Part I. Droplet nucleation radius, Int. J. Heat Mass Tran. 83 (2015) 833–841.

[20] X. Liu, P. Cheng, Dropwise condensation theory revisited Part II. Droplet nucleation density and condensation heat flux, Int. J. Heat Mass Tran. 83 (2015) 842–849.

[21] Q. Zeng, S. Xu, Thermodynamics and characteristics of heterogeneous nucleation on fractal surfaces, J. Phys. Chem. C 119 (2015) 27426–27433.

[22] T. Kimura, S. Maruyama, Molecular dynamics simulation of heterogeneous nucleation of a liquid droplet on a solid surface, Microscale Thermophys. Eng. 6 (2002) 3–13.

[23] Q. Sheng, J. Sun, Q. Wang, et al., On the onset of surface condensation: formation and transition mechanisms of condensation mode, Sci. Rep. 6 (2016) 1–9.

[24] D. Niu, L. Guo, H.W. Hu, et al., Dropwise condensation heat transfer model considering the liquid-solid interfacial thermal resistance, Int. J. Heat Mass Tran. 112 (2017) 333–342.

[25] S. Gao, Q. Liao, W. Liu, et al., Effects of solid fraction on droplet wetting and vapor condensation: a molecular dynamic simulation study, Langmuir 33 (2017) 12379–12388.

[26] S. Plimpton, Fast parallel algorithms for short-range molecular dynamics, J. Comput. Phys. 117 (1995) 1–19.

[27] F.H. Stillinger Jr., Rigorous basis of the frenkel-band theory of association equilibrium, J. Chem. Phys. 38 (1963) 1486–1494.

[28] P.E. Theodorakis, W. Paul, K. Binder, Pearl-necklace structures of molecular brushes with rigid backbone under poor solvent conditions: a simulation study, J. Chem. Phys. 133 (2010) 104901.

[29] D. Suh, K. Yasuoka, Condensation on nanorods by molecular dynamics, J. Chem. Phys. 144 (2016) 244702.